Modeling the vestibular evoked myogenic potential

Bernd Lütkenhöner, Wolfgang Stoll, T. Türker Basel

www.elsevier.com/locate/yjtbi

Modeling the vestibular evoked myogenic potential

Bernd Lütkenhöner, Wolfgang Stoll, Türker Basel

PII: S0022-5193(09)00525-6
DOI: doi:10.1016/j.jtbi.2009.10.036
Reference: YJTBI 5764

To appear in: *Journal of Theoretical Biology*

Received date: 14 May 2009
Revised date: 22 September 2009
Accepted date: 29 October 2009

Cite this article as: Bernd Lütkenhöner, Wolfgang Stoll and Türker Basel, Modeling the vestibular evoked myogenic potential, *Journal of Theoretical Biology*, doi:10.1016/j.jtbi.2009.10.036

Modeling the Vestibular Evoked Myogenic Potential

Bernd Lütkenhöner, Wolfgang Stoll, and Türker Basel

ENT Clinic, Münster University Hospital, Münster, Germany

Correspondence to:

Bernd Lütkenhöner

ENT Clinic

Kardinal-von-Galen-Ring 10

48129 Münster

Germany

Tel.: +49 251 83 56864

Fax: +49 251 83 56882

Email: Lutkenh@uni-muenster.de

Abstract

Measuring the vestibular evoked myogenic potential (VEMP) promises to become a routine method for assessing vestibular function, although the technique is not yet standardized. To overcome the problem that the VEMP amplitude depends not only on the inhibition triggered by the acoustic stimulation of the vestibular end organs in the inner ear, but also on the tone of the muscle from which the potential is recorded, the VEMP is often normalized by dividing through a measure of the electromyogram (EMG) activity. The underlying idea is that VEMP amplitude and EMG activity are proportional. But this would imply that the muscle tone is irrelevant for a successful VEMP recording, contradicting experimental evidence. Here, an analytical model is presented that allows to resolve the contradiction. The EMG is modeled as the sum of motor unit action potentials (MUAPs). A brief inhibition can be characterized by its equivalent rectangular duration (ERD), irrespective of the actual time course of the inhibition. The VEMP resembles a polarity-inverted MUAP under such circumstances. Its amplitude is proportional to both the ERD and the MUAP rate. The EMG activity, by contrast, is proportional to the square root of the MUAP rate. Thus, the normalized VEMP still depends on the muscle tone. To avoid confounding effects of the muscle tone, the standard deviation of the EMG could be considered. But the inhibition effect on the standard deviation is small so that the measuring time would have to be much longer than usual today.

Keywords: VEMP, vestibular function testing, sacculus, sonomotor responses, electromyogram, EMG

1. Introduction

Although several structural specializations have evolved within the vertebrate labyrinth that reduce the effect of ambient pressure changes on the balance organs, sufficiently loud sounds may nevertheless stimulate the vestibular end organs in the inner ear (Carey and Amin, 2006). In a report about vestibular side effects of extremely loud sounds, von Békésy (1935) speculated that the movement of the stapes might cause eddies that spread to the vestibular organs. In humans, the vestibular organ with the highest sound sensitivity seems to be the sacculus (Townsend and Cody, 1971; Todd et al., 2000; Sheykholeslami and Kaga, 2002), presumably due to its close proximity to the stapes. Other vestibular end organs appear to be acoustically responsive as well, though (see e.g. Young et al., 1977; Carey et al., 2004; Xu et al., 2009). The sacculus has bilateral excitatory connections to the neck extensor muscle motoneurons and bilateral inhibitory connections to the neck flexor muscle motoneurons (Uchino et al., 1997). Thus, stimulation of the sacculus can modulate the tonic electromyogram (EMG) activity of the respective muscles. In the averaged EMG, such modulations emerge as sonomotor responses (Jacobson and McCaslin, 2007).

The sonomotor response currently receiving the most attention is the vestibular evoked myogenic potential (VEMP) recorded from surface electrodes over the sternocleidomastoid muscle. Colebatch et al. (1994) were the first to record a response from this recording site. Clicks of 140 or 145 dB SPL were presented at a rate of 3/s while the subjects activated their neck flexors, and 512 stimulus-related epochs of surface EMG (sEMG) were averaged. The averaged sEMG, i.e. the VEMP, showed early peaks with mean latencies of 13 and 23 ms, respectively. Considering their polarity, they were denoted as p13 and n23. This pioneering work triggered not only numerous research studies, but also lead to continuously increasing clinical interest in the VEMP [see e.g. the

reviews by Ferber-Viart et al. (1999), Colebatch (2001), Welgampola and Colebatch (2005), Hamann and Haarfeldt (2006), Rauch (2006), and Jacobson and McCaslin (2007), or the recent monograph by Murofushi and Kaga (2009)]. The clinical interest results from the opinion that recording the VEMP is the only readily available method for unilaterally assessing the sacculus (Clarke et al., 2003; Wuyts et al., 2007).

The latencies of the early VEMP peaks are basically invariant, apart from a possible prolongation in the case of a retrolabyrinthine lesion (Murofushi et al., 2001). Thus, parameters of interest are mainly the amplitudes of the VEMP peaks and measures that depend on these amplitudes such as the VEMP threshold. However, the VEMP amplitude depends not only on the inhibition triggered by the acoustic stimulation of the vestibular end organs in the inner ear, but also on the level of the tonic muscle activation. Colebatch et al. (1994) quantified the latter in terms of the level of the averaged rectified sEMG that was observed just before the stimulus presentation, and they found a highly linear relationship to the VEMP amplitude. Alternatively, the muscle tone may be quantified in terms of the pre-stimulus root-mean-square (RMS) value of the sEMG, which was reported to be linearly related to the VEMP amplitude as well (Lim et al., 1995). Subsequent studies corroborated these findings (Ochi et al., 2001; Welgampola et al., 2003; Akin et al., 2004). Nowadays, the prevailing idea seems to be that the VEMP amplitude is *proportional* to the sEMG level. Many authors consequently normalize the VEMP amplitude by dividing it by a measure of the muscle tone (e.g. Karino et al., 2005; Welgampola and Colebatch, 2005; Miyamoto et al., 2006; Brantberg et al., 2007; Sandhu and Bell, 2008; Seo et al., 2008; Brantberg and Verrecchia, 2009). But there is a problem. Proportionality between VEMP amplitude and sEMG level would imply that the signal-to-noise ratio of the VEMP is independent of the muscle tone, which would be contradictory to the experience that a certain muscle tone is an indispensable requirement for a successful VEMP recording. This contradiction indicates that the relationship between VEMP amplitude and sEMG level is still insufficiently understood. The question arises as to what extent the proposed

normalization of the VEMP amplitude really eliminates the influence of the muscle tone, thus providing an unequivocal signature of the inhibition arising from the vestibular end organs.

Answering this question requires a solid theoretical basis. The theory that will be developed here was inspired by the model of Wit and Kingma (2006). They simulated the VEMP generation by adding a large number of motor unit action potentials which randomly occurred in time with equal probability, apart from a narrow time window for which complete inhibition was assumed. The theory presented below is based on a similar model, but the mathematical framework is different: Analytical formulas are derived that allow calculating the quantities of interest (mean and standard deviation of the sEMG) directly from the assumptions. The general theory requires the evaluation of integrals, but regarding a typical VEMP experiment the situation is less complicated: Approximations can be used, owing to the fact that the inhibition time window may be assumed to be short (see e.g. Colebatch and Rothwell, 2004). Thus, in the end, the question raised above can be answered on the basis of surprisingly simple formulas in an intuitively appealing way.

2. Model

2.1. Motor unit action potential and electromyogram

The elementary unit of function in the motor system is the motor unit, which consists of the cell body of the motor neuron, the axon of the motor neuron that runs in the peripheral nerve, the neuromuscular junction, and the muscle fibers innervated by that neuron (Rowland, 1991). When the motor neuron fires and an action potential reaches the neuromuscular junction, the muscle fibers depolarize and contract, and the currents associated with the depolarization spread in the surrounding volume conductor. If there were only one active motor unit, an electrode placed on the skin above the muscle would record a motor unit action potential (MUAP) whenever the unit fires.

However, under realistic conditions many motor units are simultaneously active, and the contributions of the individual motor units can barely be recognized in the recorded signal, but are intermingled in an interference pattern (Stegeman et al., 2000). This signal represents the surface electromyogram (sEMG).

The sEMG is the algebraic sum of the MUAP trains of all active motor units (Day and Hulliger, 2001). In the present study, the motor units are assumed to have the same MUAP time course, except for an amplitude factor that may differ from unit to unit. This simplifying assumption allows to integrate the MUAP trains of all motor units into a single MUAP train, where each MUAP is defined by a time of occurrence and an amplitude factor. Thus, the sEMG that is observed in a certain (finite) time range of interest may be calculated using the formula

$$v_T(t) = \sum_{i=1}^{N_T} a_i \mu(t - t_i), \tag{1}$$

where $\mu(t)$ is the time course of a normalized MUAP occurring at time zero, and t_i and a_i are time of occurrence and amplitude, respectively, of the *i*-th MUAP. The parameter N_T denotes the number of MUAPs that occur between $-T/2$ and $+T/2$, where T is assumed to be large enough to ensure that MUAPs occurring outside this range have no measurable effect on the time range of interest. The normalized MUAP, $\mu(t)$, is dimensionless, which means that the unit of measure (Volt) is attached to the amplitude factor a_i. The function $\mu(t)$ is assumed to fulfill the requirement

$$\int_{-\infty}^{+\infty} \mu(t)dt = 0 \tag{2}$$

and to have the value one at its maximum. The sample MUAP function shown in the inset of Fig. 1 (same curve also in the inset of Fig. 2A) corresponds to a single sine wave, defined as

$$\mu_{\sin e}(t) = \begin{cases} \sin(\pi t / \hat{\Delta}) & for \ -\hat{\Delta} \le t \le \hat{\Delta} \\ 0 & otherwise \end{cases}, \quad (3)$$

where $\hat{\Delta}$ is the time span between negative and positive peak. In our simulations, $\hat{\Delta}$ was 10 ms, corresponding to the interval between the peaks p13 and n23 of the VEMP. The zero crossing between the two peaks is considered as the occurrence time of the MUAP (marked by a vertical line). This special MUAP function was chosen because of its simplicity [a good alternative would have been the first derivative of a Gaussian probability density function, as in the model of Wit and Kingma (2006)]. From a physiological point of view, such a MUAP function is, of course, relatively artificial. Therefore, it is emphasized that the theory developed here does in no way depend on Eq. (3) and could easily be applied to more realistic model functions or even MUAPs actually measured. As to the latter, it must be taken into account that a MUAP is usually measured under conditions that are not comparable to a VEMP measurement. Features such as the MUAP duration strongly depend not only on the recording conditions (e.g. near- versus far-field), but also on aspects such as muscle fiber length and conduction velocity (Dumitru et al., 1999). Moreover, Eq. (1) is based on the simplifying assumption that the time course of the MUAP is identical for all motor units. Thus, $\mu(t)$ has to be interpreted as a function describing the time course of an average MUAP, which may be expected to resemble a compound muscle action potential (CMAP). The relationship between MUAP and CMAP was investigated, for example, by Dumitru (2000) and McGill et al. (2001).

To calculate an sEMG using Eq. 1, random numbers have to be generated for N_T, and for t_i and a_i ($1 \le i \le N_T$). For the times of occurrence t_i, a Poisson process with rate ρ_0 is assumed. This means that the random variable N_T has the expected value $\rho_0 T$. To simulate a real experiment, where N_T would vary from trial to trial, a random number has to be drawn from a Poisson distribution. Regarding the amplitudes a_i, Wit and Kingma (2006) suggested to use a Gamma distribution of

order 2.[1] The theory developed in the text that follows is more general, and specific assumptions about the distribution of the amplitudes are not required at this point.

2.2. Vestibular Evoked Myogenic Potential (VEMP)

With a simple extension, the above model can be transformed into a model for the VEMP. Instead of unconditionally summing over all the N_T MUAPs in Eq. 1, some of the MUAPs are considered inhibited. The inhibition is controlled by an inhibition function $\xi(t)$ that specifies the probability of inhibition.[2] Equivalently, it can be postulated that the occurrence times of the MUAPs are drawn from a time-dependent Poisson process (see e.g. Cox and Miller, 1965). This means that the probability of a MUAP between t and $t+dt$ is assumed to be $\rho(t)dt$, with a rate function

$$\rho(t) = \rho_0\big(1-\xi(t)\big). \tag{4}$$

To prevent misunderstanding it is emphasized that, if not explicitly stated otherwise, the term 'rate' refers to the ensemble of all motor units.

---

[1] In the simulations based on Eq. 1, Poisson-distributed random numbers N_T and Gamma-distributed random numbers a_i were drawn using the routines POISSRND and GAMRND, respectively, of the Matlab Statistical Toolbox (The MathWorks Inc., Natick, MA, USA). The MUAP occurrence times t_i were obtained by mapping random numbers generated by the Matlab routine RAND (uniformly distributed on the interval (0,1)) onto the time range ($-T/2$, $T/2$).

[2] Whether or not a specific MUAP in Eq. 1, say the i-th one, is considered inhibited depends on the value of $\xi(t_i)$. A value of zero means 'not inhibited', a value of one means 'inhibited'. For values in between, a random number is drawn from a uniform distribution on the interval (0,1). In our simulations, this was done using the Matlab routine RAND. Inhibition is assumed if the random number is smaller than $\xi(t_i)$. Inhibited MUAPs are excluded from the summation in Eq. 1.

Figure 1A illustrates how the sEMG arises from an interference of MUAPs. The thin curves show individual MUAPs, whereas the irregular thick curve represents their sum, i.e. the sEMG. The amplitude factors in Eq. 1, a_i, were set to 1, for the sake of simplicity. The MUAP rate was 250 s^{-1}, and complete inhibition within a 2-ms time window centered at t = 0 was assumed. A MUAP is inhibited, in the mean, every second trial under these circumstances so that the inhibition effect is negligible compared to the random fluctuations of the MUAP density. To see the inhibition effect, a sufficient number of trials are to be averaged. The white curves on black background were calculated on the basis of 500,000 trials. They show the mean and the standard deviation (STD) of the sEMG. The mean of the sEMG represents the VEMP. Except for a scaling factor, the VEMP curve is basically a polarity-inverted version of the MUAP curve shown in the inset. The STD is affected by the inhibition as well, although the effect is relatively small: At times where the absolute value of the VEMP has a maximum, the STD has a minimum. A more realistic situation is illustrated in Fig. 1B. In that simulation, the amplitude factors a_i were drawn from a Gamma distribution of order 2 rather than being constant.

Under typical experimental conditions, 200 averages suffice to obtain a VEMP with a reasonable signal-to-noise ratio. Two such examples are presented in Fig. 2. The MUAP rate was 1600 s^{-1}, and complete inhibition for a duration of 1.25 ms (Fig. 2A) and 5 ms (Fig. 2B), respectively, was assumed. The MUAPs had unit amplitude, for the sake of simplicity. The thin curves show results that were estimated on the basis of 200 trials, whereas the thick gray curves in the background represent an infinite number of trials (curves based on analytical formulas that will be derived below). As already seen in Fig. 1, the VEMP (i.e. the mean of the sEMG) is basically a polarity-inverted MUAP, except for a scaling factor (compare inset). A comparison between Figs 2A and 2B suggests that increasing the duration of the inhibition by a factor of four increases the VEMP amplitude by about the same factor. Regarding the standard deviation (STD) of the sEMG, the thin

curves in Fig. 2B show deflections similar to those in the theoretical curves (gray background). In Fig. 2A, however, the signal-to-noise ratio is insufficient.

3. Analytical considerations

Simulations based on Eq. 1 can be performed with little mathematical effort, but they are numerically expensive, because a huge number of trials have to be simulated to get estimates that approximate the expected values. Apart from that, simulations can only be done for a finite number of parameter constellations so that drawing general conclusions is problematic. This is why the model is considered analytically now. The consistency between the simulations based on Eq. 1 and the analytical model is demonstrated in Fig. 1, where the simulation results are represented by the white curves and the analytical model by the thick black curves in the background.

3.1. General theory

To prepare the transition from Eq. 1 to the analytical model, it shall be assumed that the time span T is close to infinity so that N_T may be equated with the expected number of MUAPs between $-T/2$ and $+T/2$. If the probability of a MUAP between t and $t+dt$ is $\rho(t)dt$, as postulated above, each of the N_T MUAPs in Eq. 1 occurs with the probability $\rho(t)dt / N_T$. The amplitudes a_i are assumed to be drawn independently of each other and of the MUAP occurrence times t_i. The probability that a MUAP amplitude is between a and $a+da$ is assumed to be $f(a)da$. With these assumptions, the following equation is obtained for the expected value of $v_T(t)$ in the limit $T\to\infty$:

$$\bar{v}(t) = \lim_{T\to\infty} \sum_{i=1}^{N_T} \int_0^{\infty} \int_{-T/2}^{T/2} f(a_i) \frac{\rho(t_i)}{N_T} \; a_i \mu(t - t_i) \; dt_i da_i \; . \qquad (5)$$

Simplifying this equation yields

$$\bar{v}(t) = \bar{a} \int_{-\infty}^{+\infty} \rho(t')\mu(t-t')dt', \tag{6}$$

where

$$\bar{a} = \int_{0}^{\infty} a \; f(a) \; da \tag{7}$$

is the arithmetic mean of the MUAP amplitudes. A similar formula can be derived for the variance of the sEMG (see Appendix):

$$\mathrm{var}[v(t)] = \bar{\bar{a}}^2 \int_{-\infty}^{+\infty} \rho(t')\mu^2(t-t')dt' \tag{8}$$

with

$$\bar{\bar{a}} = \sqrt{\int_{0}^{\infty} a^2 f(a) \; da} \; . \tag{9}$$

The quantity $\bar{\bar{a}}$ represents the quadratic mean of the MUAP amplitudes.

The equations 6 and 8 are more general than needed in this study. Taking into account that the rate function $\rho(t)$ has the structure specified in Eq. 4, the two equations may be rewritten as

$$\bar{v}(t) = -\rho_0 \bar{a} \int_{-\infty}^{+\infty} \xi(t')\mu(t-t')dt' \tag{10}$$

and

$$\mathrm{var}[v(t)] = \rho_0 \Delta \cdot \bar{\bar{a}}^2 \cdot (1 - \Xi(t)) \tag{11}$$

with

$$\Xi(t) = \frac{1}{\Delta} \int_{-\infty}^{+\infty} \xi(t')\mu^2(t-t')dt' . \quad (12)$$

The quantity Δ in the latter two equations is defined as

$$\Delta = \int_{-\infty}^{+\infty} \mu^2(t)dt . \quad (13)$$

It may be interpreted as a measure of the effective MUAP duration, because the integral basically measures how long the normalized MUAP has an absolute value close to the maximum value, i.e. one.

3.2. Approximations for short inhibition windows

Auditory stimuli that are used to elicit a VEMP are usually short, and the inhibition time window may be assumed to be short as well. Supposing that it is short enough to ensure that the MUAP function $\mu(t)$ is roughly constant for the duration of the inhibition, Eq. 10 may be approximated as

$$\bar{v}(t) \approx -\rho_0 \delta \cdot \bar{a}\mu(t) \quad (14)$$

with

$$\delta = \int_{-\infty}^{+\infty} \xi(t')dt' . \quad (15)$$

The latter quantity shall be called the equivalent rectangular duration (ERD) of the inhibition, because it indicates how long a rectangular window with complete inhibition must be to produce the same inhibition effect as the actual inhibition function $\xi(t)$. According to Eq. 14, the VEMP is a polarity-inverted MUAP, except for scaling issues. Its amplitude is proportional to the term $\rho_0\delta$,

which may be interpreted as the expected number of inhibited MUAPs. The approximation of $\Xi(t)$ for short inhibition windows is

$$\Xi(t) \approx \frac{\delta}{\Delta}\mu^2(t)\,. \tag{16}$$

Thus, the variance of the sEMG shows a modulation which corresponds to the MUAP function squared. The ratio δ/Δ measures the ERD in units of the effective MUAP duration.

3.3. Approximations for a slowly changing inhibition function

Very small VEMP amplitudes (or no VEMPs at all) are to be expected if the inhibition function $\xi(t)$ changes much slower than the MUAP function $\mu(t)$. Equation 10 can be approximated in that case as $\bar{v}(t) \approx 0$, due to Eq. 2. The corresponding approximation for Eq. 12 is $\Xi(t) \approx \xi(t)$. Thus, the variance of the sEMG shows a modulation which follows the time course of the inhibition.

3.4. Normalization of the VEMP

To normalize the VEMP, the recorded potential is divided by a measure of the muscle tone. Within the framework of the present theory, the most natural measure of the muscle tone is the standard deviation (or RMS value) of the uninhibited sEMG, which is $\sqrt{\rho_0\Delta}\cdot\overline{\overline{a}}$ (see Eq. 11). Normalization of the approximation for short inhibition windows (Eq. 14) yields

$$\bar{v}_{norm}(t) \approx -\frac{\rho_0\delta}{\sqrt{\rho_0\Delta}}\cdot\frac{\overline{a}}{\overline{\overline{a}}}\mu(t)\ . \tag{17}$$

The first fraction on the right of this equation was intentionally not simplified (by canceling the factor $\sqrt{\rho_0}$), because the terms in numerator and denominator have instructive interpretations: $\rho_0\delta$ is the number of inhibited MUAPs, whereas $\rho_0\Delta$ indicates with how many other MUAPs

each MUAP significantly interferes. The normalized VEMP is nothing else than a signal-to-noise ratio. The *signal* is proportional to the number of inhibited neurons, whereas the *noise* is proportional to the square root of the number of interfering MUAPs. Equation 17 shows that the normalization did not completely eliminate the dependence of the VEMP on aspects of the muscle activity. In what follows, the various factors will be considered one by one.

The dependence of the normalized VEMP on the effective MUAP duration, Δ, is not a major issue. In theory, Δ could even be estimated from the data: If it is assumed that the MUAP function $\mu(t)$ and the VEMP have a similar shape (see Eq. 14), the integral in Eq. 13 could be evaluated with a normalized MUAP function derived from the measured VEMP. But such a procedure may seriously fail if the assumption is violated. Thus, a model-based evaluation of Δ appears more appropriate. For the sine wave displayed in the inset of Fig. 1, the result is $\Delta = \hat{\Delta} = 10$ ms, corresponding to the typical latency difference of the VEMP peaks p13 and n23.

The ratio $\bar{a} / \bar{\bar{a}}$ in Eq. 17 does not represent a serious problem either, because the lack of knowledge regarding the amplitude distribution of the MUAPs can be largely compensated for by making reasonable assumptions. If the MUAP amplitudes are drawn from a Gamma distribution of order *k*, the ratio $\bar{a} / \bar{\bar{a}}$ has the value $\sqrt{k/(k+1)}$. For $k = 2$ (as in Fig. 1B) this value is 0.82, and with increasing *k* it approaches 1. Similar values can be expected for a real experiment, because the assumption of a Gamma distribution is considered appropriate for both normal and pathological conditions (e.g. Slawnych et al., 1997). All in all, the amplitude distribution of the MUAPs seems to be of secondary importance with regard to VEMP modeling. Thus, as long as the goal is to achieve a qualitative understanding of the VEMP, it appears acceptable to assume MUAPs of unit amplitude, for the sake of simplicity. This yields $\bar{a} / \bar{\bar{a}} = 1$.

The actual problem is the dependence of the normalized VEMP on the MUAP rate, ρ_0. The normalization reduced this problem, at least. Without normalization, the amplitude of the VEMP is proportional to ρ_0, whereas after normalization it is proportional to $\sqrt{\rho_0}$. Supposing, for example, that the uncertainty regarding ρ_0 corresponds to a factor of 16, the uncertainty regarding $\sqrt{\rho_0}$ corresponds to a factor of only 4.

This is illustrated in Fig. 3, which compares a situation before normalization (on the left) with a situation after normalization (on the right). Three different MUAP rates are considered: 400/s (top), 1600/s (middle), and 6400/s (bottom). Complete inhibition within a time window of 1.25 ms, centered at $t = 0$, was assumed. As in the simulations before, the MUAP function corresponded to the sine wave shown in the inset of Fig. 1. The MUAPs had unit amplitude, for the sake of simplicity. The lower curve in each panel shows the mean of the sEMG, i.e. the VEMP; the upper curve shows the standard deviation of the sEMG. The thin curves are based on 10,000 sEMG epochs (simulation using Eq. 1), whereas the thick gray curves in the background are based on the analytical solutions (Eqs 10 and 11). An increase of the MUAP rate from 400/s to 6400/s corresponds to a factor of 16. In the curves on the left, the VEMP amplitude increases by about the same factor, whereas in the normalized curves on the right there is only an increase by about a factor of 4. As to the standard deviation of the uninhibited sEMG, increasing the MUAP rate by a factor of 16 led to an increase by a factor of 4, whereas the normalized counterpart is always 1, by definition. Most interesting is the inhibition-induced modulation of the normalized standard deviation, which appears to be independent of the MUAP rate. To explain this observation, the variance of the sEMG (Eq. 11) has to be normalized. The normalized variance, i.e. the square of the normalized standard deviation, is $1 - \Xi(t)$. This term is indeed independent of the MUAP rate ρ_0 (see Eqs 12 and 16).

3.5. Relationship between VEMP amplitude and sEMG level

Both the VEMP amplitude and the standard deviation of the sEMG depend on the MUAP rate ρ_0. However, the latter is generally unknown when analyzing experimental data, and therefore it is useful to establish a more direct relationship between the two measures. The following consideration is based on the approximation for short inhibition windows, according to which the peak amplitude of the VEMP has an absolute value of

$$s = \rho_0 \delta \cdot \overline{a} \,. \tag{18}$$

The standard deviation of the uninhibited sEMG is

$$\sigma = \sqrt{\rho_0 \Delta} \cdot \overline{\overline{a}} \,. \tag{19}$$

The latter formula may be rewritten as $\rho_0 = \sigma^2 / \left(\Delta \overline{\overline{a}}^2\right)$. Inserting this result into the equation for *s* yields:

$$\frac{s}{\overline{a}} = \frac{\delta}{\Delta} \cdot \frac{\sigma^2}{\overline{\overline{a}}^2} \tag{20}$$

Thus, the VEMP amplitude is proportional to the variance of the sEMG. If both quantities are appropriately normalized (division by $\overline{a}$ and $\overline{\overline{a}}^2$, respectively), the factor of proportionality is the ratio of ERD and effective MUAP duration.

4. Discussion

4.1. Resolving a seeming contradiction

Starting point for this theoretical study was the realization that the common view of a proportional relationship between VEMP amplitude and sEMG level (in this study quantified in terms of the standard deviation of the sEMG, σ) is contradictory to the experience that a successful VEMP recording requires a certain muscle tone. Equation 20 allows to resolve the contradiction, although this is not obvious at first glance. The importance of the muscle tone follows from the fact that, according to Eq. 20, s/σ is proportional to σ. This means the higher the muscle tone, the better is the signal-to-noise ratio of the VEMP. However, the equation appears to conflict with the view that VEMP amplitude and sEMG level are proportional to each other. Instead, it suggests that the VEMP amplitude is proportional to the sEMG level squared. This raises the question as to why contradictory conclusions were drawn from experimental data.

The pivotal element in the following consideration is the ERD, δ. So far, there was no reason to address the question as to how δ might depend on experimental conditions. But this question becomes crucially import now. By reanalyzing data published in the classical article by Colebatch et al. (1994) it will be exemplified how the parameter δ can be used to reconcile model and experiment. Data points read from Fig. 4B of that article are displayed as filled circles in Fig. 4A. A linear fit (thick gray line in the background) is quite satisfactory so that the data could be seen as counterevidence to the quadratic law suggested by Eq. 20. But such a conclusion would be premature. The dashed curve shows a quadratic function fitted to all data points with a mean sEMG level <70 µV (4 data points excluded). The function explains these data at least as well as the linear function.

To remove the discrepancy between model and data at higher sEMG levels, the inhibition function $\xi(t)$ is assumed to depend on the MUAP rate ρ_0. The inhibition function determines the *proportion* of MUAPs that are inhibited, and it appears reasonable to assume that the relative inhibition effect decreases with increasing excitation. In Eq. 20, the inhibition effect is not expressed in terms of the inhibition function $\xi(t)$, but in terms of the ERD δ, which is an integral of the inhibition function (Eq. 15). In order to make the model consistent with the data, δ is assumed to be a function of σ:

$$\delta(\sigma) = \frac{\delta_0}{\sqrt{1+\sigma^2/\sigma_{ref}^2}} \qquad (21)$$

With this empirical extension, the model explains the data also at higher sEMG levels (black solid curve). The estimated reference sEMG level was σ_{ref} = 37.5 µV. At low sEMG levels, Eq. 21 may be approximated as $\delta(\sigma) \approx \delta_0$, and the VEMP amplitude is proportional to σ^2 (dotted curve). At high sEMG levels, Eq. 21 may be approximated as $\delta(\sigma) \approx \delta_0 \sigma_{ref}/\sigma$ so that the VEMP amplitude becomes proportional to σ. The latter approximation explains why the curve representing the model basically coincides, over a wide range of levels, with the linear fit published by Colebatch et al. (1994). The curve in Fig. 4B shows the function $\delta(\sigma)/\delta_0$, which shall be called the relative ERD. If the muscle tone is high, the relative ERD is about five times smaller than if the muscle tone is low.

The normalized VEMP is considered in Fig. 4C. Data points and curves were derived from the counterparts in Fig. 4A by dividing the p13-n23 amplitude by the mean sEMG activity. The normalized VEMP linearly increases with the sEMG activity if the latter is low (dotted line). At intermediate levels, where the majority of the data points are found, this increase slows down, and beyond a level of 60 µV the normalized VEMP is roughly independent of the sEMG activity.

4.2. Estimation of the ERD

The above considerations exemplified how to compare different experimental conditions by calculating *relative* ERDs. At least in theory, the data of a VEMP experiment allow to determine the ERD in *absolute* terms, too. This information is not contained in the classical VEMP curve (mean of the sEMG), but requires inspecting the standard deviation of the sEMG (as explained in the context of Fig. 3). Getting meaningful data for such an analysis may be a challenging task, though. The problem is that the standard deviation is affected to a much lesser degree by the inhibition than the mean (see Fig 2A). Thus, to make an analysis of the standard deviation possible, the measuring time has to be largely increased. This appears feasible in scientific investigations, where data could also be accumulated over multiple sessions and subjects, if necessary. Whether estimating the ERD could become an option for clinical investigations as well is difficult to assess at this point. Figure 2B suggests that not more than 200 sEMG trials are required to obtain clear evidence of an inhibition effect in the standard deviation. In a real experiment, however, an ERD of 5 ms, as assumed in that example, might be difficult to achieve.

4.3. Estimation of the MUAP rate

Given the ERD, another quantity of potential interest could be determined as well: the MUAP rate ρ_0. By combining Eqs 18 and 19, an equation for s/σ can be obtained. Solving this equation for ρ_0 yields

$$\rho_0 = \frac{\Delta}{\delta^2} \cdot \frac{s^2}{\sigma^2} \cdot \frac{\overline{\overline{a}}^2}{\overline{a}^2} \ . \tag{22}$$

This equation will be used now to estimate the order of magnitude of the MUAP rate in a typical VEMP experiment. The assumptions $\Delta = 10$ ms and $\left(\overline{\overline{a}}/\overline{a}\right)^2 = 3/2$ are based on considerations

presented above. The assumption s/σ = 3/5 implies that the average of 100 trials has a signal-to-noise ratio of 6 (assuming that averaging n trials enhances the signal-to-noise ratio by $\sqrt{n}$), which seems to be a realistic order of magnitude for a typical VEMP experiment. Considering the inhibition effects found in peristimulus time histograms of motor unit discharges (Colebatch and Rothwell, 2004), the assumption δ = 2 ms appears to be reasonable. With these assumptions, Eq. 22 predicts a MUAP rate of 1350/s. This value is consistent with an estimate derived by Wit and Kingma (2006). Referring to Keenan et al. (2005) they assumed that the number of motor units contributing to the sEMG recorded from the sternocleidomastoid muscle is between 50 and 100. Moreover, referring to a compilation of MUAP rates in a review article by Enoka and Fuglevand (2001) they assumed a MUAP rate of 25/s per motor unit. For the ensemble of all contributing motor units they consequently estimated a MUAP rate between 1250/s and 2500/s.

5. Conclusions

Building upon the pioneering work of Wit and Kingma (2006), an analytical model has been developed that explains the VEMP by the inhibition of MUAPs. An inhibition that is short compared to the duration of the VEMP (a reasonable assumption, considering e.g. the study of Colebatch and Rothwell, 2004) can be characterized in terms of its ERD, irrespective of its actual time course. In theory, the ERD can be estimated from measured data by considering the standard deviation of the sEMG. But in practice, this is problematic because the inhibition effect on the standard deviation is small. Thus, the measuring time would have to be much longer than usual today.

For an ERD being independent of the sEMG level, the VEMP amplitude predicted by the model is proportional to the *variance* of the sEMG. The *normalized* VEMP amplitude, defined as the ratio of VEMP amplitude and standard deviation of the sEMG, is consequently proportional to the *standard*

deviation of the sEMG. Since the normalized VEMP amplitude may be interpreted as a signal-to-noise ratio, the model explains why a certain muscle tone is an indispensable requirement for a successful VEMP recording. The model is also able to explain why experimental data often suggest a more or less proportional relationship between VEMP amplitude and sEMG level (quantified, for example, by the RMS value of the sEMG). For that purpose, it has to be assumed that the ERD decreases with increasing sEMG level, which means that the relative inhibition effect (proportion of inhibited MUAPs) is assumed to diminish with increasing excitation. All in all, the model suggests that the optimal condition for measuring the VEMP is an intermediate muscle tone. Increasing the muscle tone to the highest possible level would cause discomfort without significantly enhancing the signal-to-noise ratio.

6. Appendix: Variance of the sEMG

The variance of $v_T(t)$ in the limit $T \to \infty$ may be calculated as

$$\mathrm{var}[v(t)] = \lim_{T\to\infty} E\left[v_T^2(t)\right] - \left(\bar{v}(t)\right)^2, \qquad \text{(A1)}$$

where E[…] denotes the expected value. To calculate the first term on the right of this equation, $v_T^2(t)$ is expanded, yielding

$$E\left[v_T^2(t)\right] = E\left[\sum_{i=1}^{N_T} a_i^2 \mu^2(t-t_i)\right] + 2\cdot E\left[\sum_{i=1}^{N_T-1}\sum_{j=i+1}^{N_T} a_i a_j \mu(t-t_i)\mu(t-t_j)\right]. \qquad \text{(A2)}$$

Evaluation of the second term in Eq. A2 yields

$$2\sum_{i=1}^{N_T-1}\sum_{j=i+1}^{N_T}\int_0^{\infty}\int_0^{\infty}\int_{-T/2}^{T/2}\int_{-T/2}^{T/2}\frac{\rho(t_i)}{N_T}\frac{\rho(t_j)}{N_T}f(a_i)f(a_j)\;a_i a_j\mu(t-t_i)\mu(t-t_j)\;dt_i dt_j da_i da_j\,,$$

which can be rewritten as

$$\frac{N_T^2-N_T}{N_T^2}\left(\bar{a}\int_{-T/2}^{T/2}\rho(t')\mu(t-t')dt\right)^2.$$

In the limit $T\to\infty$, N_T is negligible compared to N_T^2, and, with Eq. 6, the above term reduces to

$$\left(\bar{a}\int_{-\infty}^{+\infty}\rho(t')\mu(t-t')dt'\right)^2=\left(\bar{v}(t)\right)^2.$$

Using this result, Eq. A1 may be rewritten as

$$\mathrm{var}[v(t)]=\lim_{T\to\infty}E\left[\sum_{i=1}^{N_T}a_i^2\mu^2(t-t_i)\right]. \qquad \text{(A3)}$$

The remaining calculation is analogous to the calculation of $\bar{v}(t)$. The result is Eq. 8.

References

Akin, F.W., Murnane, O.D., Panus, P.C., Caruthers, S.K., Wilkinson, A.E. and Proffitt, T.M. (2004) The influence of voluntary tonic EMG level on the vestibular-evoked myogenic potential. J Rehabil Res Dev 41, 473-80.

Brantberg, K., Granath, K. and Schart, N. (2007) Age-related changes in vestibular evoked myogenic potentials. Audiol Neurootol 12, 247-53.

Brantberg, K. and Verrecchia, L. (2009) Testing vestibular-evoked myogenic potentials with 90-dB clicks is effective in the diagnosis of superior canal dehiscence syndrome. Audiol Neurootol 14, 54-8.

Carey, J. and Amin, N. (2006) Evolutionary changes in the cochlea and labyrinth: Solving the problem of sound transmission to the balance organs of the inner ear. Anat Rec A Discov Mol Cell Evol Biol 288, 482-9.

Clarke, A.H., Schönfeld, U. and Helling, K. (2003) Unilateral examination of utricle and saccule function. Journal of Vestibular Research 13, 215-225.

Colebatch, J.G., Halmagyi, G.M. and Skuse, N.F. (1994) Myogenic potentials generated by a click-evoked vestibulocollic reflex. J Neurol Neurosurg Psychiatry 57, 190-7.

Colebatch, J.G. (2001) Vestibular evoked potentials. Curr Opin Neurol 14, 21-6.

Colebatch, J.G. and Rothwell, J.C. (2004) Motor unit excitability changes mediating vestibulocollic reflexes in the sternocleidomastoid muscle. Clin Neurophysiol 115, 2567-73.

Cox, D.R. and Miller, H.D. (1965) *The theory of stochastic processes* Chapman and Hall, London.

Day, S.J. and Hulliger, M. (2001) Experimental simulation of cat electromyogram: evidence for algebraic summation of motor-unit action-potential trains. J Neurophysiol 86, 2144-58.

Dumitru, D., King, J.C. and Zwarts, M.J. (1999) Determinants of motor unit action potential duration. Clin Neurophysiol 110, 1876-82.

Dumitru, D. (2000) Physiologic basis of potentials recorded in electromyography. Muscle Nerve 23, 1667-85.

Enoka, R.M. and Fuglevand, A.J. (2001) Motor unit physiology: some unresolved issues. Muscle Nerve 24, 4-17.

Ferber-Viart, C., Dubreuil, C. and Duclaux, R. (1999) Vestibular evoked myogenic potentials in humans: a review. Acta Otolaryngol 119, 6-15.

Hamann, K.F. and Haarfeldt, R. (2006) Vestibulär evozierte myogene Potentiale. HNO 54, 415-426.

Jacobson, G.P. and McCaslin, D.L. (2007) The vestibular evoked myogenic potential and other sonomotor evoked potentials. In: Burkard, R.F., Eggermont, J.J., Don, M. (Eds.), *Auditory Evoked Potentials - Basic Principles and Clinical Applications.* Lippincott Williams & Wilkins, Philadelphia, pp. 572-598.

Karino, S., Ito, K., Ochiai, A. and Murofushi, T. (2005) Independent effects of simultaneous inputs from the saccule and lateral semicircular canal. Evaluation using VEMPs. Clin Neurophysiol 116, 1707-15.

Keenan, K.G., Farina, D., Maluf, K.S., Merletti, R. and Enoka, R.M. (2005) Influence of amplitude cancellation on the simulated surface electromyogram. J Appl Physiol 98, 120-31.

Lim, C.L., Clouston, P., Sheean, G. and Yiannnikas, C. (1995) The influence of voluntary EMG activity and click intensity on the vestibular click evoked myogenic potential. Muscle & Nerve 18, 1210-1213.

McCue, M.P. and Guinan, J.J., Jr. (1997) Sound-evoked activity in primary afferent neurons of a mammalian vestibular system. Am J Otol. 18, 355-60.

McGill, K.C., Lateva, Z.C. and Xiao, S. (2001) A model of the muscle action potential for describing the leading edge, terminal wave, and slow afterwave. IEEE Trans Biomed Eng 48, 1357-65.

Miyamoto, A., Seo, T., Node, M., Hashimoto, M. and Sakagami, M. (2006) Preliminary study on vestibular-evoked myogenic potential induced by bone-conducted stimuli. Otol Neurotol 27, 1110-4.

Murofushi, T. and Curthoys, I.S. (1997) Physiological and anatomical study of click-sensitive primary vestibular afferents in the guinea pig. Acta Otolaryngol 117, 66-72.

Murofushi, T., Shimizu, K., Takegoshi, H. and Cheng, P.W. (2001) Diagnostic value of prolonged latencies in the vestibular evoked myogenic potential. Arch Otolaryngol Head Neck Surg 127, 1069-72.

Murofushi, T. and Kaga, K. (2009) *Vestibular Evoked Myogenic Potential - Its Basics and Clinical Applications* Springer, Tokyo.

Ochi, K., Ohashi, T. and Nishino, H. (2001) Variance of vestibular-evoked myogenic potentials. Laryngoscope 111, 522-7.

Rauch, S.D. (2006) Vestibular evoked myogenic potentials. Curr Opin Otolaryngol Head Neck Surg 14, 299-304.

Rowland, L.P. (1991) Diseases of the motor unit. In: Kandel, E.R., Schwartz, J.H., Jessell, T.M. (Eds.), *Principles of neural science*, 3rd ed. Appleton & Lange, Norwalk, CT, pp. 244-257.

Sandhu, J.S. and Bell, S.L. (2008) Effects of eye position on the vestibular evoked myogenic potential. Acta Otolaryngol, 1-4.

Seo, T., Miyamoto, A., Saka, N., Shimano, K., Nishida, T., Hashimoto, M. and Sakagami, M. (2008) Vestibular evoked myogenic potential induced by bone-conducted stimuli in patients with conductive hearing loss. Acta Otolaryngol 128, 639-43.

Sheykholeslami, K. and Kaga, K. (2002) The otolithic organ as a receptor of vestibular hearing revealed by vestibular-evoked myogenic potentials in patients with inner ear anomalies. Hear Res 165, 62-7.

Slawnych, M., Laszlo, C. and Hershler, C. (1997) Motor unit number estimation: sample size considerations. Muscle Nerve 20, 22-8.

Stegeman, D.F., Blok, J.H., Hermens, H.J. and Roeleveld, K. (2000) Surface EMG models: properties and applications. J Electromyogr Kinesiol 10, 313-26.

Todd, N.P., Cody, F.W. and Banks, J.R. (2000) A saccular origin of frequency tuning in myogenic vestibular evoked potentials? Implications for human responses to loud sounds. Hear Res 141, 180-8.

Townsend, G.L. and Cody, D.T. (1971) The averaged inion response evoked by acoustic stimulation: its relation to the saccule. Ann Otol Rhinol Laryngol 80, 121-31.

Uchino, Y., Sato, H., Sasaki, M., Imagawa, M., Ikegami, H., Isu, N. and Graf, W. (1997) Sacculocollic reflex arcs in cats. J Neurophysiol 77, 3003-12.

von Békésy, G. (1935) Über akustische Reizung des Vestibularapparates. Pflügers Archiv European Journal of Physiology 236, 59-76.

Welgampola, M.S., Rosengren, S.M., Halmagyi, G.M. and Colebatch, J.G. (2003) Vestibular activation by bone conducted sound. J Neurol Neurosurg Psychiatry 74, 771-8.

Welgampola, M.S. and Colebatch, J.G. (2005) Characteristics and clinical applications of vestibular-evoked myogenic potentials. Neurology 64, 1682-8.

Wit, H.P. and Kingma, C.M. (2006) A simple model for the generation of the vestibular evoked myogenic potential (VEMP). Clin Neurophysiol 117, 1354-8.

Wuyts, F.L., Furman, J., Vanspauwen, R. and Van de Heyning, P. (2007) Vestibular function testing. Curr Opin Neurol 20, 19-24.

Figure Captions

Fig. 1 Model explaining how surface electromyogram (sEMG) and vestibular evoked myogenic potential (VEMP) arise from motor unit action potentials (MUAPs). The sEMG (irregular thick curve) is the algebraic sum of MUAPs randomly distributed along the time axis (thin curves; **inset** showing single MUAP). The MUAP rate was 250/s. The MUAP generation was inhibited in a 2-ms window centered at time zero, but this assumption has no obvious effect on a single sEMG trial. The mean of 500,000 sEMG trials (lower white curve on black background), by contrast, looks like a polarity-inverted MUAP. This curve represents the VEMP. The inhibition effect can also be seen in the standard deviation (STD) of the sEMG (upper white curve on black background). **A** All MUAP amplitudes were identical. **B** The MUAP amplitudes were drawn from a Gamma distribution of order 2.

Fig. 2. VEMPs for inhibition windows of 1.25 ms **(A)** and 5 ms **(B)**, respectively. The thin curves were calculated on the bases of 200 simulated sEMG trials; the thick gray curves in the background represent analytical solutions. The lower curves show the VEMP (mean of the sEMG), whereas the upper curves show the standard deviation (STD) of the sEMG. The MUAPs had unit amplitude; they occurred at a rate of 1600/s. **Inset:** MUAP waveform, for the sake of comparison.

Fig. 3: VEMP (lower curve) and standard deviation of the sEMG (upper curve) before and after normalization for three different MUAP rates: 400/s (top), 1600/s (middle), and 6400/s (bottom). The inhibition window had a duration of 1.25 ms. The thin curves are based on 10,000 sEMG epochs; the gray curves in the background represent analytical solutions.

Fig. 4: Reanalysis of the data in Colebatch et al.'s (1994) figure 4B. **A** VEMP amplitude (amplitude difference between the peaks p13 and n23) versus mean sEMG activity. The filled circles show the data read from the original paper; the thick gray line in the background represents a linear fit to the data. The data points with a mean sEMG level <70 μV can also be explained by a quadratic function (dashed curve). The black curve represents a function that is quadratic in the limit of low sEMG levels (dotted curve), but linear in the limit of high sEMG levels. **B** Relative ERD as a function of the mean sEMG activity. **C** Normalized VEMP amplitude versus mean sEMG activity. Data points and curves were derived from the counterparts in Fig. 4A by dividing the p13-n23 amplitude by the mean sEMG activity.

Fig. 1

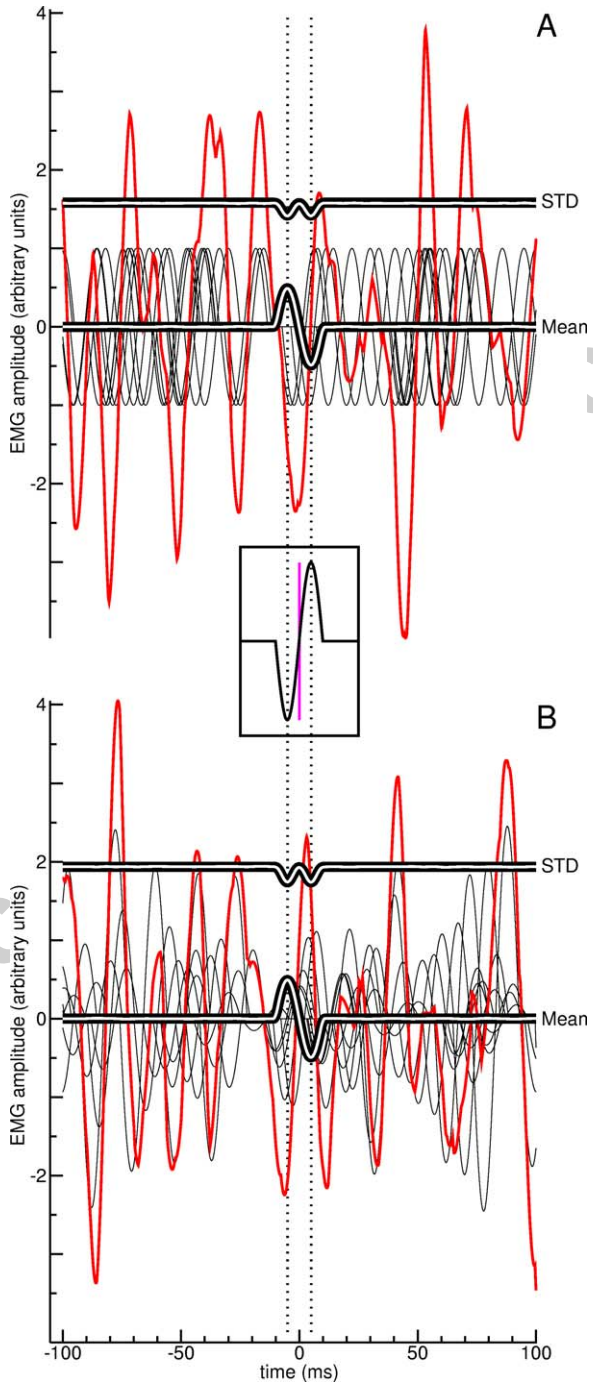

Fig. 2

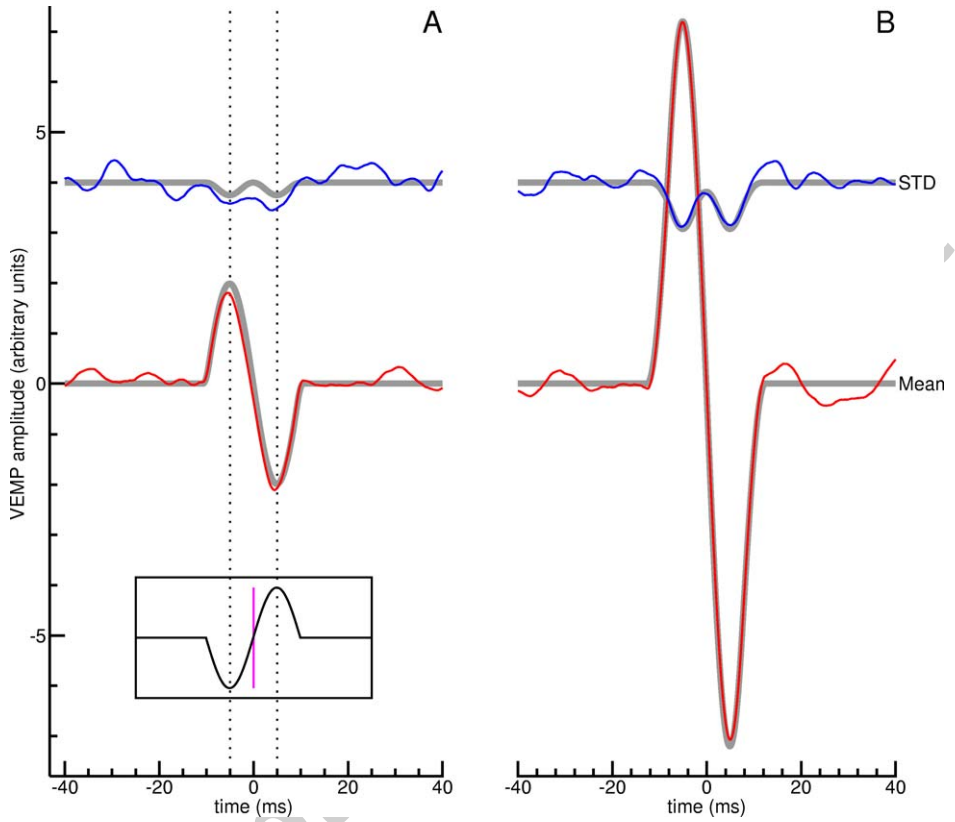

Fig. 3

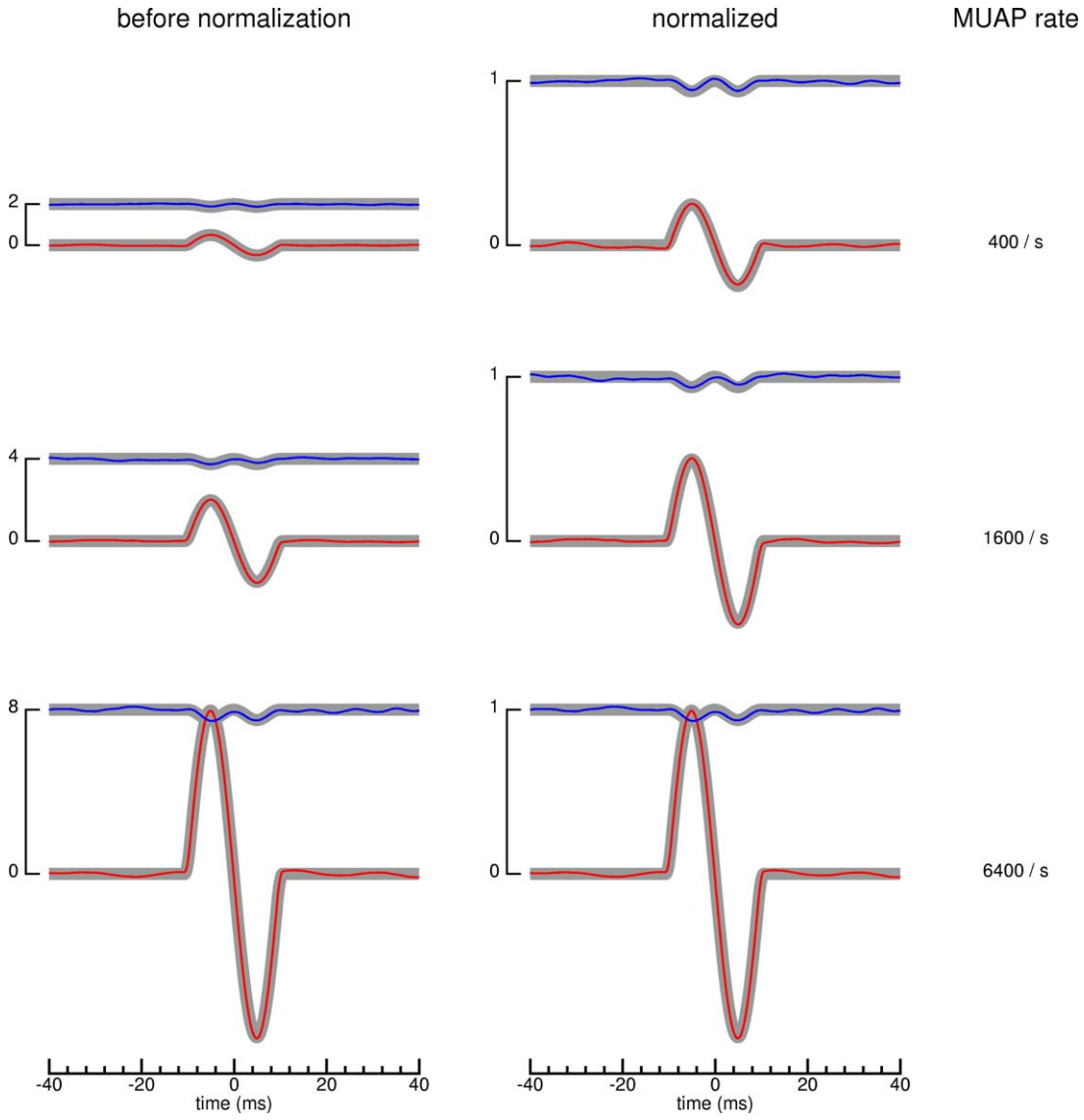

Fig. 4